Nanostructures

DOI: 10.1002/ange.200600239

Platinum-Functionalized Octahedral Silica Nanocages: Synthesis and Characterization**

*Xiong Wen Lou, Chongli Yuan, Qing Zhang, and Lynden A. Archer**

The preparation of hollow inorganic micro- and nanostructures has attracted consistent research efforts in the last few years.[1–22] The technological importance of these hollow particles are well-demonstrated in a myriad of applications, including their use as nanoscale chemical reactors, efficient catalysts, drug-delivery carriers, photonic building blocks, and energy-storage media.[1–17] The general approach for the preparation of hollow particles involves the use of various

[*] X. W. Lou, C. Yuan, Q. Zhang, Prof. Dr. L. A. Archer
School of Chemical and Biomolecular Engineering
Cornell University
Ithaca, NY 14853-5201 (USA)
Fax: (+1) 607-255-9166
E-mail: laa25@cornell.edu

[**] We are grateful to the National Science Foundation (DMR-0404278) for supporting this study. Facilities available through the Cornell Center for Materials Research (CCMR), a Materials Research Science and Engineering Center of the National Science Foundation (DMR-0079992), were used for this study.

removable templates, including hard structures such as narrow size-distribution silica[1,2] and polymer–latex spheres,[7–9] as well as soft ones, for example, emulsion droplets,[10] micelles,[11] and even gas bubbles.[12] More-novel approaches based on the Kirkendall effect[14,15,19] and galvanic replacement[16] are also employed to construct hollow particles. Nonetheless, the geometry of hollow structures obtained from these approaches is primarily spherical.

The construction of hollow particles with other well-defined shapes is still a significant challenge to materials scientists. Several recent efforts devoted to the synthesis of nonspherical hollow micro- and nanostructures have produced promising results. Sun and Xia constructed single-crystal cubic Au/Ag-alloy nanoboxes with Ag nanocubes as sacrificial templates,[16a] as well as Pd nanoboxes by utilizing a simple and elegant corrosion-based method.[17] PbTe nanoboxes were synthesized by using a one-pot solvothermal route.[18] Highly symmetric 18-faceted polyhedral nanocages of Cu_7S_4 were prepared by treating precursor cubic Cu_2O nanocrystals with thiourea at 90 °C.[19] Furthermore, Yang and Zeng reported a one-pot solution synthesis of polycrystalline hollow SnO_2 octahedra in relatively high yield, based on the 2D aggregation of nanocrystallites.[20] Most recently, single-crystal octahedral Cu_2O nanocages were prepared through a one-pot catalytic solution process,[21] and hollow polyaniline with octahedral morphology was also prepared with presynthesized octahedral Cu_2O templates.[22]

Despite these successes, a simple general strategy for the synthesis of nonspherical hollow particles is preferred. Herein we propose a potentially general approach towards the facile synthesis of hollow particles with octahedral and other (e.g. cubic) morphology. We demonstrate the concept by preparing octahedral silica nanocages. Silica is chosen because of the intrinsic simplicity of its sol-gel chemistry.[8,9,23]

The synthetic strategy is as follows: $[H_2PtCl_6]$ is added to a mixture of ethanol/H_2O/ammonia containing tetraethylorthosilicate (TEOS) and aminopropyltrimethoxysilane (APS) to form a yellow precipitate of $[(NH_4)_2PtCl_6]$ instantaneously. This is followed by surface functionalization in situ with the amino groups from APS, which plays an important role in the subsequent deposition of silica on the $[(NH_4)_2PtCl_6]$ quasi-template (see below). This quasitemplate method has several important advantages over conventional template strategies. First, the quasitemplates, though insoluble in the original ethanol/H_2O reaction mixture, are easily removed by washing with water. Moreover, the template is generated in situ, which renders presynthesized hard templates unnecessary, thus allowing structures with a wider range of sizes and of extremely high purity to be synthesized readily. Furthermore, the quasitemplate itself is the precursor to noble-metal nanoparticles, which can lead to controlled Pt-functionalized products by simple calcination.

Figure 1 shows some silica nanostructures produced by the above procedure. The materials depicted were obtained after intensive washing with water to produce better TEM visualization. Even after several cycles of washing, we found that trace amounts of the Pt precursor remained. From the low-magnification image (Figure 1 d), it is apparent that the main reaction product is the targeted octahedral silica nanocages, with a much smaller amount of featureless silica particles (dark spots in the figure) produced by homogeneous nucleation. Although the morphological yield of octahedral structures was high (> 90 %), the size of these structures spanned a wide range, from 200 nm to 1.5 μm, with the vast majority in the range of 500 nm to 1 μm. Control experiments without APS produced a much lower yield of octahedral silica structures, thus underscoring its importance in the synthesis. The octahedral morphology of the silica structures can be clearly seen in the high-magnification images (Figure 1 a, c), with all eight facets being equilateral triangles. Figure 1 e shows a high-magnification field-emission scanning-electron-microscopy (FESEM) image, which again confirms unambiguously that the particles are indeed octahedral and hollow. Interestingly, twinning of two octahedra (Figure 1 b) through edge- or plane-sharing is often observed as reported for other octahedral particles.[20–22]

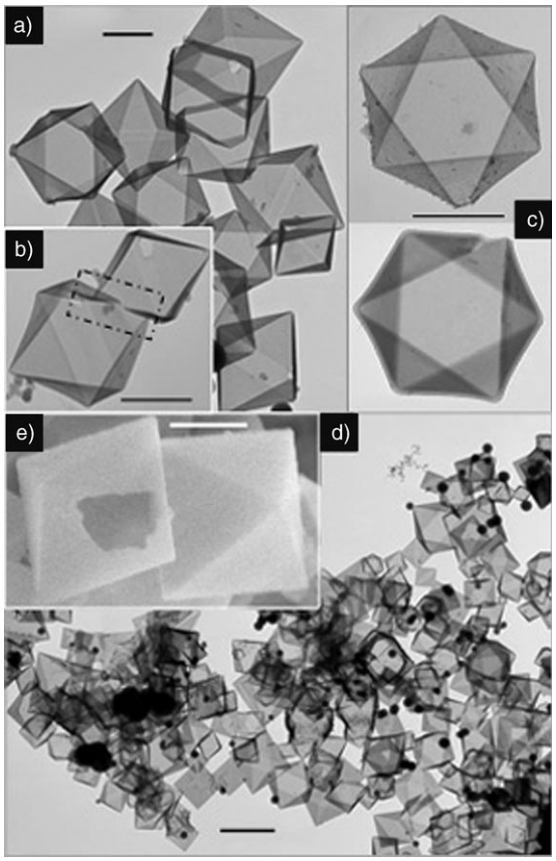

Figure 1. a)–d) TEM images and e) FESEM image of octahedral silica nanostructures after intensive washing with water. b) Two plane-sharing twinned octahedra; c) two free-standing octahedra clearly showing that each plane is an equilateral triangle; d) typical low-magnification overall view of octahedra, in which the darker spots are silica spheres; e) a perfect octahedron and a broken hollow octahedron. The scale bar in d) is 2 μm, all the rest are 500 nm.

Figure 2 shows the powder XRD patterns of the product (washed only with ethanol) a) before and b) after calcination at 450 °C. All peaks in a) and b) can be indexed undisputedly to cubic $[(NH_4)_2PtCl_6]$ (JCPDS card 07-0218) and cubic Pt (JCPDS card 04-0802), respectively. The elemental composi-

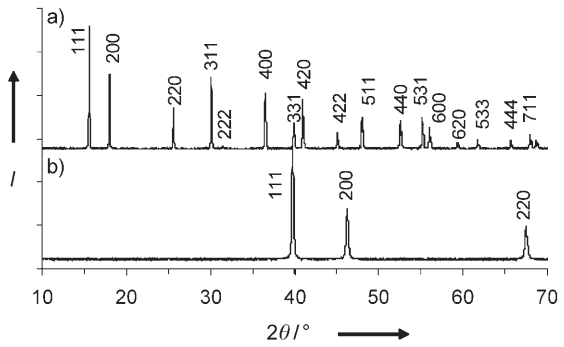

Figure 2. XRD patterns of the same product a) before and b) after calcination at 450 °C for 1 h. The product was washed with ethanol only.

tions of the products were confirmed with energy-dispersive X-ray (EDX) analysis (see below). Thermogravimetric analysis (TGA) revealed a sharp weight loss at 300–350 °C, which corresponds to the decomposition of $[(NH_4)_2PtCl_6]$ to form metallic Pt. The products after calcination were further examined with TEM. It was found that the octahedral morphology remained essentially intact (Figure 3). The wall thickness was 20–40 nm as estimated from Figure 3c and e.

Another interesting observation is that depending on the amount of Pt precursor that remains in the product after washing, the size and distribution of the Pt nanoparticles trapped inside the octahedral nanocages can be controlled. For example, when the $[(NH_4)_2PtCl_6]$ was partially removed by washing with water before calcination, the resultant Pt nanoparticles were relatively small (< 100 nm) and uniformly distributed on the interior walls (Figure 3a–c). In contrast, without prior removal by washing with water, the Pt precursor decomposed to form a few big particles (Figure 3e, f), which appeared to congregate around one apex of the structures (Figure 3e). In this way, controlled functionalization with Pt in the interior of nanocages could be achieved. Furthermore, it is well-known that the silica shell formed through the Stöber process is highly porous, evidence for which is provided in this case by the easy removal of $[(NH_4)_2PtCl_6]$ in water.[8,9,23] These pores could serve as percolated channels that connect the interior cavity and exterior space for potential applications such as nanoreactors.[4,5,20]

Detailed composition characterization was carried out with EDX analysis and converged-beam electron diffraction (CBED). Measurements based on nanostructures that contain a small number of Pt nanoparticles are particularly revealing because they facilitate spatially resolved characterization of the composition of individual units. Specifically, EDX spectra were collected from different locations within the nanostructures (Figure 4). From the EDX spectrum (Figure 4b) corresponding to spot 1 (Figure 4a, b inset), it is clear that the bright mushroomlike particle in the dark-field TEM image (Figure 4a, marked with a white square) is composed of Pt, and that these particles are trapped inside a silica cage, with their crystalline nature confirmed by CBED (Figure 4a inset). If the X-ray beam is positioned slightly off spot 1 (i.e. spot 2 or any other dark area within the nanostructure, e.g. spot 3), the EDX spectrum (Figure 4c) shows much stronger silica bands and no hint of Pt, thus indicating that the material is locally composed of silica.

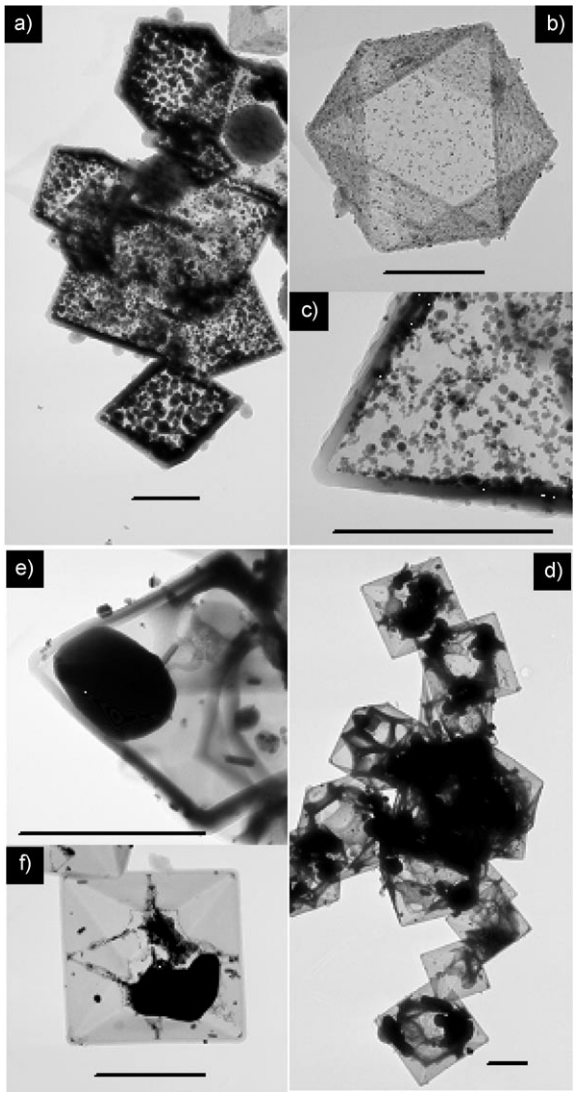

Figure 3. TEM images of Pt-functionalized silica nanocages. a)–c) The Pt precursor in the product was partially removed by washing with water prior to calcination; d)–f) the product was washed with ethanol only so that no Pt precursor was removed before calcination. All scale bars are 500 nm.

To understand further the proposed mechanism by which octahedral nanocages are formed, several control experiments were conducted. For example, if mixture B (silica precursor; see Experimental Section) was not added, only microsized $[(NH_4)_2PtCl_6]$ octahedra were formed (Figure 5a). The octahedral shape may therefore be intrinsically attributed to its cubic crystal structure, for which the formation of {111} surface planes is favorable.[20,21] The inset in Figure 5a reveals another important feature: Most of the surface of the eight {111} planes of larger crystals (about 10 μm) is absent. This is likely due to inefficient monomers during rapid crystal growth, which leads to preferential growth at the edges. On the other hand, smaller crystals (< 5 μm) have only some hexagonal windows on their {111} planes, which may even be

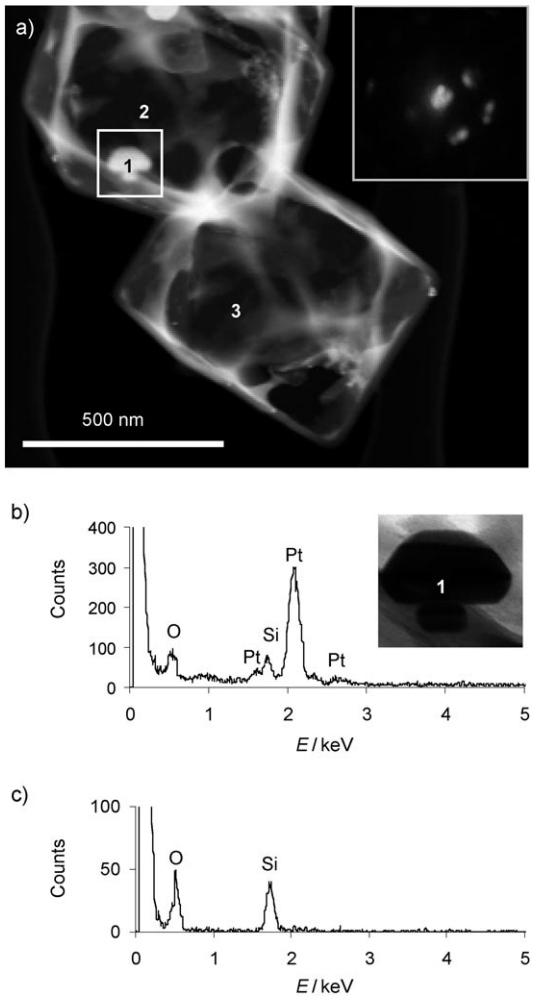

Figure 4. a) Dark-field TEM image; the inset shows a typical CBED pattern with clear diffraction spots from small Pt nanoparticles; b) EDX spectrum collected from spot 1 in a); the inset shows a magnified bright-field TEM image of spot 1; c) typical EDX spectrum collected from a dark area such as spot 2 and spot 3 in a).

completely closed to form perfect octahedra. The crystal-growth behavior could be largely altered in the presence of silica sols and the functionalizing APS; the formation of larger octahedral skeletons is inhibited, whereas the growth of small perfect octahedra is favored. To gain more insight, we also reversed the sequence in which mixture B and $[H_2PtCl_6]$ were introduced. The product consisted of large skeleton-like octahedra, many small perfect octahedra, and a significant fraction of silica spheres (Figure 5b). Notably, the large octahedron is assembled from six small octahedra, which may provide clues about the prevention of growth of larger octahedra and the origin of twinning between the individual structures.

Although the construction scheme reported herein is a one-step process, successful preparation of octahedral nanocages of a particular size or range of sizes is evidently the result of fine-tuning many other experimental conditions such as the hydrolysis rate of TEOS and the amount of APS required for optimal deposition. The proposed facile strategy for the preparation of octahedral nanostructures can be

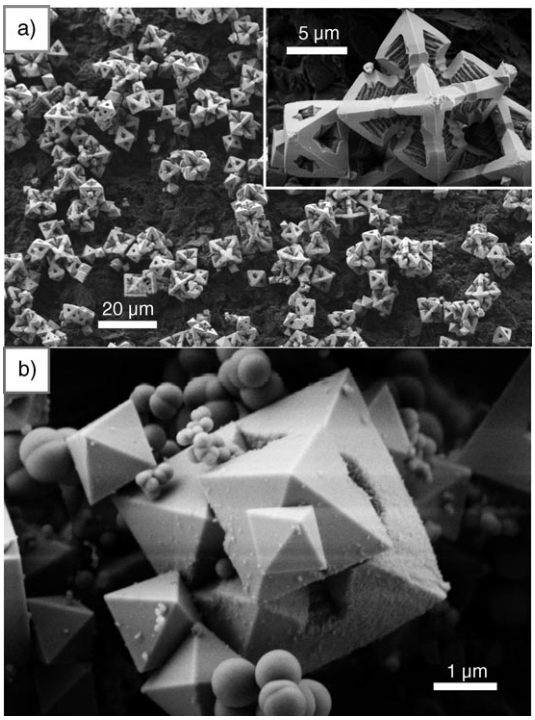

Figure 5. FESEM images of $[(NH_4)_2PtCl_6]$ microcrystals a) produced without adding mixture B (silica precursor) and b) obtained by reversing the order in which mixture B and $[H_2PtCl_6]$ were added (see Experimental Section).

extended to other polyhedra and materials such as metal oxides. Our continual effort is directed towards the construction of polyhedral nanocages for TiO_2, ZrO_2, and composites.

In summary, octahedral silica nanocages have been prepared by a facile one-step approach, which also enabled controlled functionalization with Pt in the cavities. The strategy is based on mediated deposition of silica on simultaneously generated salt quasitemplates, which can be simply removed by washing with water. By suitable optimization of the sol-gel chemistry, the growth mechanism can, in principle, be implemented in the synthesis of hollow polyhedra of many other materials.

Experimental Section

Mixture A, composed of absolute ethanol (58.5 g), deionized water (10 g), and ammonia (29.6%, 3 g), and mixture B, composed of TEOS (99%, 3 mL; Aldrich) and APS (0.4 mL; Gelest), were prepared as stock solutions. Pt-functionalized octahedral silica nanocages were synthesized by APS-assisted deposition of silica on insoluble quasi-templates generated in situ. Mixture B (20 µL) and hydrogen hexachloroplatinate(IV) solution (8 wt% in H_2O, 300 µL; Aldrich) were added successively to mixture A (2 mL) within about 3 s under vigorous magnetic stirring; a yellow precipitate was formed instantaneously. The resulting mixture was quickly vortexed for 10 s and kept under static conditions for 1 h. The solid product was harvested by centrifugation and washed with ethanol, deionized water, and again with ethanol, before being vacuum-dried at room temperature. The yellow $[(NH_4)_2PtCl_6]$ is insoluble in ethanol but soluble in water, so the amount of Pt in the final product can be controlled by the number of washing cycles with water. The dried product was calcined at 450 °C for 1 h to give Pt-functionalized octahedral silica nanocages.

Products were characterized with powder XRD analysis (Scintag PAD X, $Cu_{K\alpha}$, $\lambda = 1.5406$ Å), EDX spectroscopy (JEOL 8900 EPMA Microprobe), TEM (JEOL-1200EX, 120 kV), ultrahigh-vacuum scanning TEM (100 kV) equipped with EDX analysis and CBED, and FESEM (LEO 1550, 3 kV).

Received: January 19, 2006
Published online: April 28, 2006

Keywords: nanocages · nanostructures · platinum · silica · template synthesis

[1] a) F. Caruso, R. A. Caruso, H. Möhwald, *Science* **1998**, *282*, 1111; b) F. Caruso, *Adv. Mater.* **2001**, *13*, 11.
[2] Y. F. Zhu, J. L. Shi, W. H. Shen, X. P. Dong, J. W. Feng, M. L. Ruan, Y. S. Li, *Angew. Chem.* **2005**, *117*, 5213; *Angew. Chem. Int. Ed.* **2005**, *44*, 5083.
[3] S. W. Kim, M. Kim, W. Y. Lee, T. Hyeon, *J. Am. Chem. Soc.* **2002**, *124*, 7642.
[4] H. P. Liang, H. M. Zhang, J. S. Hu, Y. G. Guo, L. J. Wan, C. L. Bai, *Angew. Chem.* **2004**, *116*, 1566; *Angew. Chem. Int. Ed.* **2004**, *43*, 1540.
[5] a) J. Li, H. C. Zeng, *Angew. Chem.* **2005**, *117*, 4416; *Angew. Chem. Int. Ed.* **2005**, *44*, 4342; b) H. G. Yang, H. C. Zeng, *J. Phys. Chem. B* **2004**, *108*, 3492.
[6] Q. Liu, H. Liu, M. Han, J. Zhu, Y. Liang, Z. Xu, Y. Song, *Adv. Mater.* **2005**, *17*, 1995.
[7] a) M. Yang, J. Ma, C. Zhang, Z. Yang, Y. Lu, *Angew. Chem.* **2005**, *117*, 6885; *Angew. Chem. Int. Ed.* **2005**, *44*, 6727; b) Z. Z. Yang, Z. W. Niu, Y. F. Lu, Z. B. Hu, C. C. Han, *Angew. Chem.* **2003**, *115*, 1987; *Angew. Chem. Int. Ed.* **2003**, *42*, 1943.
[8] Y. Lu, J. McLellan, Y. N. Xia, *Langmuir* **2004**, *20*, 3464.
[9] X. W. Lou, C. Yuan, E. Rhoades, Q. Zhang, L. A. Archer, *Adv. Funct. Mater.*, in press.
[10] H. G. Yang, H. C. Zeng, *Angew. Chem.* **2004**, *116*, 5318; *Angew. Chem. Int. Ed.* **2004**, *43*, 5206.
[11] C. I. Zoldesi, A. Imhof, *Adv. Mater.* **2005**, *17*, 924.
[12] Q. Peng, Y. Dong, Y. Li, *Angew. Chem.* **2003**, *115*, 3135; *Angew. Chem. Int. Ed.* **2003**, *42*, 3027.
[13] X. Sun, Y. Li, *Angew. Chem.* **2004**, *116*, 3915; *Angew. Chem. Int. Ed.* **2004**, *43*, 3827.
[14] Y. D. Yin, R. M. Rioux, C. K. Erdonmez, S. Hughes, G. A. Somorjai, A. P. Alivisatos, *Science* **2004**, *304*, 711.
[15] J. Yang, L. Qi, C. Lu, J. Ma, H. Cheng, *Angew. Chem.* **2005**, *117*, 604; *Angew. Chem. Int. Ed.* **2005**, *44*, 598.
[16] a) Y. G. Sun, Y. N. Xia, *Science* **2002**, *298*, 2176; b) Y. Sun, B. Mayers, Y. Xia, *Adv. Mater.* **2003**, *15*, 641.
[17] Y. Xiong, B. Wiley, J. Chen, Z. Y. Li, Y. Yin, Y. Xia, *Angew. Chem.* **2005**, *117*, 8127; *Angew. Chem. Int. Ed.* **2005**, *44*, 7913.
[18] W. Wang, B. Poudel, D. Wang, Z. F. Ren, *Adv. Mater.* **2005**, *17*, 2110.
[19] H. Cao, X. Qian, C. Wang, X. Ma, J. Yin, Z. Zhu, *J. Am. Chem. Soc.* **2005**, *127*, 16024.
[20] H. G. Yang and H. C. Zeng, *Angew. Chem.* **2004**, *116*, 6056; *Angew. Chem. Int. Ed.* **2004**, *43*, 5930.
[21] C. Lu, L. Qi, J. Yang, X. Wang, D. Zhang, J. Xie, J. Ma, *Adv. Mater.* **2005**, *17*, 2562.
[22] Z. Zhang, J. Sui, L. Zhang, M. Wan, Y. Wei, L. Yu, *Adv. Mater.* **2005**, *17*, 2854.
[23] W. Stöber, A. Fink, E. Bohn, *J. Colloid Interface Sci.* **1968**, *26*, 62.

